
Bayesian Diagnostics in a Skew-Normal Autoregressive Model

Authors: YONGHUI LIU

– School of Statistics and Data Science,
Shanghai University of International Business and Economics,
China
liuyh@lsec.cc.ac.cn

ANQI XIE

– School of Statistics and Data Science,
Shanghai University of International Business and Economics,
China
xaq13576743659@163.com

CHENGCHENG HAO

– School of Statistics and Data Science,
Shanghai University of International Business and Economics,
China
chengcheng.hao@suibe.edu.cn

MICHEL VAN DE VELDEN 

– Econometric Institute, Erasmus University Rotterdam,
the Netherlands
vandevelden@ese.eur.nl

SHUANGZHE LIU  

– Faculty of Science and Technology, University of Canberra,
Australia
shuangzhe.liu@canberra.edu.au

Received: Month 0000

Revised: Month 0000


Accepted: Month 0000

Abstract:

- Autoregressive modeling is a crucial tool in time series analysis, finding extensive applications in various fields. This paper explores Bayesian statistical diagnostics for a skew-normal autoregressive model. Initially, a Markov Chain Monte Carlo algorithm, combining Gibbs sampling and Metropolis-Hastings, is utilized for parameter estimation of the model. Subsequently, different perturbation schemes are established for the priors, variances, and data, employing Bayes factor, ϕ divergence, and posterior mean as measures of perturbation for Bayesian local influence analysis. Numerical simulations and comparative studies are conducted to demonstrate the effectiveness and superiority of the diagnostics. Finally, the diagnostic model is applied to empirical analysis of the daily log returns series of the Shanghai Composite Index in 2015.

Keywords:

- *Bayesian local influence; Bayesian perturbation; MCMC algorithm; Skew-normal autoregressive model.*

 Corresponding author

AMS Subject Classification:

- 62M10, 62F15, 62F35.

1. INTRODUCTION

Autoregressive modeling is very important in various fields including economics and finance, commonly used for forecasting and analyzing time series data such as stock prices, exchange rates, and economic indicators. Extensive results on the estimation, diagnostics and applications of AR models can be found in e.g. [Box et al. \(2015\)](#) and [Liu et al. \(2020a\)](#).

Statistical diagnostics is essential in data analysis, with the main task of assessing the adequacy of a given model fit to known observed data. Since the introduction of the concept of local influence by [Cook \(1986\)](#), numerous studies have been conducted on its application, see e.g. [Lawrance \(1988\)](#), [Lesaffre and Verbeke \(1998\)](#), [Liu \(2000, 2004\)](#), [Paula et al. \(2012\)](#), [Liu et al. \(2015, 2017, 2020b, 2022a,b, 2024b\)](#), [Zhu et al. \(2015, 2016\)](#), [Saavedra-Nievas et al. \(2023\)](#), [Cárcamo et al. \(2024\)](#), [Su et al. \(2024\)](#) and [Dang et al. \(2025\)](#). However, for certain complex data and models, computing the corresponding density function can be extremely challenging, making it difficult to implement statistical diagnostic methods based on the log-likelihood function. It was not until [Zhu and Lee \(2001\)](#) proposed a statistical diagnostic model based on the EM algorithm that the use of the Q-function, instead of the log-likelihood function, for handling missing data became feasible. [Liu et al. \(2020b, 2022b\)](#) and others have used this method for statistical diagnostics. With advancements in technology and computing, and insights from prior information, Bayesian analysis has become a viable approach. In Bayesian analysis we can effectively integrate prior knowledge with observed data, thereby enhancing the accuracy and reliability of our analytical results. By incorporating prior information, Bayesian analysis often demonstrates surprising outcomes in tasks such as small-sample inference, uncertainty quantification, and missing data treatment. It finds applications in various fields, including medical diagnosis, financial risk assessment, artificial intelligence decision-making, among others. Therefore, building upon Cook's perturbation method, [McCulloch \(1989\)](#) extended the Bayesian local influence approach to assess the impact of perturbations in prior or likelihood. Subsequently, [Zhu et al. \(2011\)](#) developed a more general framework for Bayesian local influence analysis, propelling it into a new stage of development. [Dai et al. \(2019\)](#) developed a Bayesian local influence framework for spatial autoregressive models with heteroscedasticity, enhancing diagnostic techniques for time series. Similarly, [Ju et al. \(2018, 2022\)](#) advanced Bayesian local influence methods for skew-normal spatial dynamic panel and autoregressive models, offering robust diagnostic tools for time series and spatial data analysis.

Initially, financial returns was assumed to follow a normal distribution. However, extensive findings have highlighted the non-normality, heavy tails, and negative skewness observed in empirical distributions of financial returns, as discussed by e.g. [Fama \(1965\)](#), [Peiro \(1999\)](#), [Chen et al. \(2005\)](#) and [Liu et al. \(2024b\)](#). As a result, [Azzalini \(1985, 2013\)](#) proposed the skew-normal distribution as a more suitable alternative for describing financial returns. It can better capture the asymmetric distribution, peaks, and fat-tail phenomena in financial

time series, be more flexible in simulating extreme events, and better align with the volatility and risk characteristics of the actual market. This perspective has been further emphasized by Carmichael and Coën (2013) and Liu et al. (2020b, 2022b, 2024b) in addressing asset pricing issues and using the skew-normal distribution for analyzing stock return data.

Regarding the estimation and diagnostics of AR models, the frequentist approach has evolved from maximum likelihood estimation and Cook's distance to the use of the EM algorithm and normal curvature for diagnostics, as exemplified by Cao et al. (2014), Maleki and Arellano-Valle (2017) and Liu et al. (2022b). However, to the best of our knowledge, there is currently no diagnostic method for the SNAR model within the Bayesian framework. Considering the broader application of SNAR models in financial time series, exploring diagnostic methods for SNAR models in the Bayesian paradigm has become very meaningful. To assess the performance of Bayesian diagnostics in a SNAR model, we employ a similar approach to that in Zhu et al. (2011), constructing a Bayesian perturbation manifold to measure the magnitude of perturbation in the Bayesian perturbation model.

The structure of the remaining of this paper is as follows: Section 2 introduces the SNAR model and the MCMC algorithm for parameter estimation. Section 3 presents the process of Bayesian local influence analysis for the SNAR model, including the Bayesian perturbation model, perturbation ensemble, and local influence measurement. Section 4 conducts effectiveness simulations and compares the Bayesian local influence analysis with local influence analysis. Section 5 consists of empirical studies. Finally, Section 6 makes our conclusion.

2. SNAR Model and MCMC Algorithm

In this section, we consider the SNAR model, studied in Liu et al. (2020b, 2022b), and use the MCMC algorithm to compute the estimated values of the parameters.

Let Y follow a skew-normal distribution with location ($\mu \in \mathbb{R}$), scale ($\sigma > 0$) and skewness ($\lambda \in \mathbb{R}$), denoted as $Y \sim \mathcal{SN}(\mu, \sigma^2, \lambda)$. Azzalini (1985, 2013) believes that skewed normal distributions possess some interesting properties. That is $E(Y) = \mu + \sigma\delta\sqrt{2/\pi}$ and $\text{Var}(Y) = \sigma^2 - (2/\pi)\sigma^2\delta^2$ with $\delta = \lambda/\sqrt{1+\lambda^2}$. Further, Y has the following random expression:

$$Y = \mu + \sigma\delta H + \sigma\sqrt{(1-\delta^2)}H_1,$$

where $H = |H_0|$, and H_0 and H_1 are two independent standard normal distributions. Moreover,

$$(2.1) \quad Y|H = h \sim \mathcal{N}\left(\mu + \frac{\lambda\sigma}{\sqrt{1+\lambda^2}}h, \frac{\sigma^2}{1+\lambda^2}\right),$$

where H follows the half normal distribution, $H \sim \mathcal{HN}(0, 1)$.

In this paper, we consider a skewed autoregressive model $\text{SNAR}(p)$:

$$(2.2) \quad Y_t = \mathbf{x}_t^\top \boldsymbol{\beta} + u_t, \quad t = p+1, \dots, T,$$

where Y_t is a time series, $\mathbf{x}_t = (Y_{t-1}, \dots, Y_{t-p})^\top$ is a $p \times 1$ vector, $\boldsymbol{\beta} = (\beta_1, \dots, \beta_p)^\top$ is a $p \times 1$ regression coefficient vector, u_t is the error following a skew-normal distribution and

$\boldsymbol{\theta} = (\boldsymbol{\beta}, \lambda, \sigma)^\top$ is the $(p + 2) \times 1$ vector of parameters. For estimating the parameters in SNAR models, frequentist approaches typically use the EM algorithm, see Liu et al. (2020b). In contrast, Bayesian approaches often employ variational inference or MCMC algorithms for sampling, see Makowski et al. (2002). Due to the non-standard form of the posterior distribution of some parameters in SNAR models, we consider using a combination of Gibbs sampling and Metropolis-Hastings algorithm for parameter estimation.

Firstly, to obtain the posterior distribution of the unknown parameters $\boldsymbol{\theta} = (\boldsymbol{\beta}, \lambda, \sigma)$ in the SNAR model, it is necessary to specify appropriate prior distributions. Following the approach of McCulloch and Tsay (1994), we adopt the following priors:

$$\boldsymbol{\beta} \sim \mathcal{N}(\mu_\beta, \Sigma_\beta), \quad \lambda \sim \mathcal{N}(\mu_\lambda, \sigma_\lambda^2), \quad \sigma \sim \chi^2(n),$$

where $\mu_\beta, \mu_\lambda, \Sigma_\beta, \sigma_\lambda$ and n are known hyperparameters.

Assuming independence among these parameters a priori, by Bayes' theorem we derive the full conditional posterior distributions of the parameters as follows:

(1) The full conditional posterior distribution of $\boldsymbol{\beta}$ is

$$(2.3) \quad p(\boldsymbol{\beta}|Y, \lambda, \sigma) \propto \exp\left\{-\frac{1}{2}(\boldsymbol{\beta} - M_\beta)^T \Omega_\beta^{-1}(\boldsymbol{\beta} - M_\beta)\right\},$$

where $\Omega_\beta^{-1} = \Sigma_\beta^{-1} + \frac{1+\lambda^2}{\sigma^2} \sum_{t=p+1}^T x_t x_t^T$ and $M_\beta = \Omega_\beta^{-1} \left\{ \Sigma_\beta^{-1} \mu_\beta + \frac{1+\lambda^2}{\sigma^2} \sum_{t=p+1}^T x_t \left(y_t - \frac{\lambda\sigma}{\sqrt{1+\lambda^2}} h \right) \right\}$.

(2) The full conditional posterior distribution of λ is

$$(2.4) \quad p(\lambda|Y, \boldsymbol{\beta}, \sigma) \propto (\sqrt{1+\lambda^2})^{T-p} \exp\left\{-\frac{(\lambda - \mu_\lambda)^2}{2\sigma_\lambda^2}\right\} \prod_{t=p+1}^T \exp\left\{-\frac{1+\lambda^2}{2\sigma^2} \left(y_t - \mathbf{x}_t^\top \boldsymbol{\beta} - \frac{\lambda\sigma}{\sqrt{1+\lambda^2}} h \right)^2\right\}.$$

(3) The full conditional posterior distribution of σ is

$$(2.5) \quad p(\sigma|Y, \boldsymbol{\beta}, \lambda) \propto \sigma^{\frac{n}{2}-1-(T-p)} \exp\left\{-\frac{\sigma}{2}\right\} \prod_{t=p+1}^T \exp\left\{-\frac{1+\lambda^2}{2\sigma^2} \left(y_t - \mathbf{x}_t^\top \boldsymbol{\beta} - \frac{\lambda\sigma}{\sqrt{1+\lambda^2}} h \right)^2\right\}.$$

After deriving the approximate posterior parameter distribution, we consider sampling the parameter $\boldsymbol{\beta}$ using the Gibbs algorithm. Since the full conditional posterior distributions of parameters λ and σ are not familiar standard distributions, we employ the Metropolis-Hastings algorithm (MCMC¹) to simulate posterior samples of the parameters. This combined algorithm generates samples over 10,000 iterations by iteratively updating the parameters. We discard the initial 50% of parameter samples, considering it as a ‘‘burn-in’’ phase. The resulting sequence of parameter samples is denoted as $\boldsymbol{\theta}^{(n)}$, from which we compute the mean to derive the parameter estimate.

¹The focus of this paper is on Bayesian statistical diagnostics for the model; therefore, details regarding Bayesian parameter estimation are not elaborated. The parameter estimation in this article is computed using Python code. Alternatively, one may consider employing the ‘RStan’ or the ‘PYMC’ package in Python for Bayesian parameter estimation.

3. Perturbation Schemes

3.1. Perturbation models

As in [Zhu et al. \(2011\)](#), we introduce a perturbation model $p(y, \theta|\omega) = p(\theta|\omega_p)p(y|\theta, \omega_d, \omega_s)$ to account for potential anomalies in the prior assumptions (w_p), model specification (w_s), and data (w_d). Therefore, the overall perturbed form can be expressed as $\omega = (\omega_p, \omega_d, \omega_s)$, $\omega = \omega_p + \omega_d + \omega_s$, and $\omega^0 = (\omega_p^0, \omega_d^0, \omega_s^0) \in \mathbb{R}^m$ represents the unperturbed case.

The perturbed model $\mathcal{M} = p(y, \theta|\omega) : \omega \in \mathbb{R}^m$ forms an m -dimensional manifold under some regular conditions. The tangent space \mathcal{T}_ω of \mathcal{M} at each $\omega \in \mathcal{M}$ is spanned by m functions $\partial_{\omega_k} \ell(\omega)$, where $\ell(\omega) = \log p(y, \theta|\omega)$ and $\partial_{\omega_k} = \partial/\partial\omega_k$, ω_k is the k -th value of ω , $k = 1, \dots, m$. So, under some regular rules

$$g_{jk}(\omega) = E_\omega \{ \partial_{\omega_j} \ell(\omega) \partial_{\omega_k} \ell(\omega) \} = -E_\omega \{ \partial_{\omega_j \omega_k}^2 \ell(\omega) \}, \quad j, k = 1, \dots, m$$

forms the measurement tensor of \mathcal{M} , and E_ω is the expectation of the joint probability density $p(y, \theta|\omega)$.

We denote $\mathbf{G}(\omega) = \{g_{jk}(\omega)\}$, where the j -th element $g_{jj}(\omega)$ of $\mathbf{G}(\omega)$ represents the magnitude of perturbation caused by ω_j , while $g_{jk}(\omega)$ characterizes the correlation between ω_j and ω_k . We aim to find suitable perturbations that make $\mathbf{G}(\omega)$ a diagonal matrix. According to [Zhu et al. \(2011\)](#), we obtain the following perturbations and derive the computation of the tangent space \mathcal{T}_ω and the diagonal matrix \mathbf{G} of SNAR(p) under different perturbation models.

3.1.1. Perturbation of priors

In order to construct a perturbation model for SNAR based on Bayesian theory, we follow the assumptions proposed in Section 2 to set the prior information. Specifically, we assume that $\beta \sim \mathcal{N}(\mu_\beta, \sigma_\beta^2)$, $\lambda \sim \mathcal{N}(\mu_\lambda, \sigma_\lambda^2)$ and $\sigma \sim \chi^2(n)$. Through the expression of the perturbation model, we can clearly see that the prior perturbation is independent of the data perturbation and the variance perturbation. This independence allows us to consider the perturbations of the priors and data or the priors and variances simultaneously. Therefore, we first propose a prior perturbation model for the parameter $\theta = (\beta, \lambda, \sigma)$. The model is constructed by introducing a small perturbation into the prior distribution, aiming to more accurately simulate the uncertainty and variability of the parameters, and its corresponding kernel function is as follows:

$$\begin{aligned} p(y, \theta|\omega) &= p(\theta|\omega) \cdot p(y|\theta) \\ &\propto p(\theta|\omega) \\ &\propto \exp \left\{ \sum_{i=1}^p \frac{(\beta_i - \mu_{\beta_i} - \omega_{\beta_i})}{2\sigma_{\beta_i}^2} \right\} \cdot \exp \left\{ \frac{\lambda - \mu_\lambda - \omega_\lambda}{2\sigma_\lambda^2} \right\} \cdot \frac{\sigma^{((n-\omega_\sigma)/2-1)}}{2^{(n-\omega_\sigma)/2} \Gamma \left(\frac{(n-\omega_\sigma)}{2} \right)} \end{aligned}$$

where $\omega_{p+2} = (\omega_\beta, \omega_\lambda, \omega_\sigma)$, $\omega_{p+2}^0 = (0, 0, \dots, 0)$ represents the case without disturbances. The perturbation model $\mathcal{M} = \{p(y, \theta|\omega) : \omega \in R^{p+2}\}$ forms a Riemannian manifold, and the tangent vector space \mathcal{T}_ω spanned by \mathcal{M} is:

$$(3.1) \quad \begin{aligned} \partial_\omega l(\omega)|_{\omega=\omega_0} &= \left(\frac{\beta_1 - \mu_{\beta_1}}{\sigma_{\beta_1}^2}, \dots, \frac{\beta_p - \mu_{\beta_p}}{\sigma_{\beta_p}^2}, \frac{\lambda - \mu_\lambda}{\sigma_\lambda^2}, \frac{1}{2} \ln \frac{2}{\sigma} + \frac{1}{2} \frac{d\Gamma(\frac{n}{2})}{d(\frac{n}{2})} \right), \\ G(\omega_0) &= \text{diag} \left(\frac{1}{\sigma_{\beta_1}^2}, \dots, \frac{1}{\sigma_{\beta_p}^2}, \frac{1}{\sigma_\lambda^2}, \int \left(\frac{1}{2} \ln \frac{2}{\sigma} + \frac{1}{2} \frac{d\Gamma(\frac{n}{2})}{d(\frac{n}{2})} \right)^2 p(y, \theta|\omega^0) dy d\theta \right) \end{aligned}$$

3.1.2. Perturbation of standard deviations (sd's)

In the Bayesian local influence framework, we consider applying a minor perturbation to the SNAR model by scaling the original standard deviation σ_t by a time-varying factor ω_t , with a new standard deviation $\sigma_t \times \omega_t$ obtained. The purpose of this perturbation is to examine the influence of variations on the posterior distribution of the SNAR model. By incorporating this perturbation, we can obtain an updated posterior distribution that incorporates the adjustments made to the standard deviation, and its corresponding kernel function is as follows:

$$\begin{aligned} p(y, \theta|\omega) &= p(y|\theta, \omega_s)p(\theta) \\ &\propto p(y|\theta, \omega_s) \\ &\propto \exp \left\{ - \sum_{t=p+1}^T \left(\log\left(\frac{\sigma_t}{\omega_t}\right) + \frac{(1+\lambda^2)\omega_t^2}{2\sigma_t^2} \left(y_t - \mathbf{x}_t^\top \boldsymbol{\beta} - \frac{\lambda\sigma_t}{\sqrt{1+\lambda^2}\omega_t} h \right)^2 \right) \right\} \\ &\propto \exp \left\{ - \sum_{t=p+1}^T \left(\log\left(\frac{\sigma_t}{\omega_t}\right) + \frac{(1+\lambda^2)\omega_t^2}{2\sigma_t^2} \left(u_t - \frac{\lambda\sigma_t}{\sqrt{1+\lambda^2}\omega_t} h \right)^2 \right) \right\}, \end{aligned}$$

where $\omega_{T-p}^0 = (1, 1, \dots, 1)$ represents the case without perturbation.

The perturbation model $\mathcal{M} = \{p(y, \theta|\omega_s) : \omega \in R^{T-p}\}$ forms a Riemannian manifold, and the tangent vector space \mathcal{T}_ω spanned by \mathcal{M} is as follows:

$$(3.2) \quad \begin{aligned} \partial_\omega l(\omega)|_{\omega=\omega_0} &= \left(1 - \frac{1+\lambda^2}{\sigma^2} \left(u_{p+1} - \frac{\lambda\sigma}{\sqrt{1+\lambda^2}} h \right)^2 - \frac{\lambda h}{\sigma} \left(u_{p+1} - \frac{\lambda\sigma}{\sqrt{1+\lambda^2}} h \right) \sqrt{1+\lambda^2}, \right. \\ &\dots, \left. 1 - \frac{1+\lambda^2}{\sigma^2} \left(u_T - \frac{\lambda\sigma}{\sqrt{1+\lambda^2}} h \right)^2 - \frac{\lambda h}{\sigma} \left(u_T - \frac{\lambda\sigma}{\sqrt{1+\lambda^2}} h \right) \sqrt{1+\lambda^2} \right), \\ G(\omega_0) &= \text{diag} (2 + \lambda^2, 2 + \lambda^2, \dots, 2 + \lambda^2). \end{aligned}$$

3.1.3. Perturbation of data

In this paper, we not only consider perturbations to the variance of the data distribution but also explore the impact of perturbing the data itself. However, our approach to data perturbation differs from the method proposed in Liu et al. (2022b). We use $y_t + \omega_t$ instead of y_t , which modifies the dataset while preserving its overall structure. This enables us to evaluate the sensitivity and robustness of the model to different perturbations applied to the input data. By employing this perturbation scheme, we can obtain updated posterior distributions that reflect the influence of these data variations on the AR model.

$$\begin{aligned}
p(y, \theta | \omega) &= p(y | \theta, \omega_d) p(\theta) \\
&\propto p(y | \theta, \omega_d) \\
&\propto \exp \left\{ - \sum_{t=p+1}^T \frac{(1 + \lambda^2)}{2\sigma^2} \left(y_t - \mathbf{x}_t^\top \boldsymbol{\beta} - \frac{\lambda\sigma}{\sqrt{1 + \lambda^2}} h - \omega_t \right)^2 \right\} \\
&\propto \exp \left\{ - \sum_{t=p+1}^T \frac{(1 + \lambda^2)}{2\sigma^2} \left(u_t - \frac{\lambda\sigma}{\sqrt{1 + \lambda^2}} h - \omega_t \right)^2 \right\},
\end{aligned}$$

where $\omega_{T-p}^0 = (0, 0, \dots, 0)$ represents the case without perturbation. The perturbation model $\mathcal{M} = \{p(y, \theta | \omega_s) : \omega \in R^{T-p}\}$ forms a Riemannian manifold, and the tangent vector space \mathcal{T}_ω spanned by \mathcal{M} is:

$$\begin{aligned}
(3.3) \quad \partial_\omega l(\omega) |_{\omega=\omega_0} &= \left(\frac{(1+\lambda^2)}{\sigma^2} \left(u_{p+1} - \frac{\lambda\sigma}{\sqrt{1+\lambda^2}} h \right), \dots, \frac{(1+\lambda^2)}{\sigma^2} \left(u_T - \frac{\lambda\sigma}{\sqrt{1+\lambda^2}} h \right) \right), \\
G(\omega_0) &= \text{diag} \left(\frac{1+\lambda^2}{\sigma^2}, \dots, \frac{1+\lambda^2}{\sigma^2} \right).
\end{aligned}$$

3.2. Local influence

In the field of time series, Liu et al. (2017) have studied outlier detection using the local influence analysis proposed by Cook (1986). However, the traditional local influence methods may not meet the requirements of Bayesian models. At this point, Zhu et al. (2011) introduced the Bayesian local influence framework, which we will validate as the basis for our analysis and discussion, specifically focusing on its effectiveness in time series models.

Let's consider a function $f(\omega) : \mathcal{M} \rightarrow \mathbb{R}^l$, where \mathcal{M} is a finite-dimensional manifold and $f(\omega)$ is a one-dimensional objective function. Suppose $\omega(t)$ is a measurement on \mathcal{M} , $\omega(0) = \omega^0$ and $\partial_t \omega(t) |_{t=0} = h \in R^m$. By Taylor expansion, we have $f(\omega(t)) = f(\omega(0)) + f'_h(0)t + O(t^2)$, where $f'_h(0) = \nabla_f^\top \mathbf{h}$ and $\nabla_f = \partial_\omega f(\omega(0))$. Next, we briefly review the important theories in Zhu et al. (2011) to provide a theoretical basis for the subsequent simulations, which mainly include two impact measures and three objective functions.

3.2.1. First-order influence measure

Firstly, consider the case $\nabla_f \neq 0$. In this situation, the first-order influence (FI) measure in the direction of $\mathbf{h} \in \mathcal{R}^m$ is defined as follows:

$$FI_{f,\mathbf{h}} = FI_{f(\omega(0)),\mathbf{h}} = \frac{\mathbf{h}^\top \nabla_f W_f \nabla_f^\top \mathbf{h}}{\mathbf{h}^\top \mathbf{G} \mathbf{h}},$$

where $\mathbf{G} = \mathbf{G}(\omega^0)$, W_f is a semi-positive matrix. For the appropriate perturbation $\tilde{\omega}$, $FI_{f,\mathbf{h}}$ can also be written as

$$FI_{f(\tilde{\omega}),\mathbf{h}}|_{\tilde{\omega}=\omega^0} = \frac{\mathbf{h}^\top \mathbf{G}^{-1/2} \nabla_f W_f \nabla_f^\top \mathbf{G}^{-1/2} \mathbf{h}}{\mathbf{h}^\top \mathbf{h}},$$

The larger the value of $FI_{f,\mathbf{h}}$, the greater the local impact it has on the statistical model. Furthermore, in order to assess $FI_{f(\omega_0),\mathbf{h}}$ objectively, we take the following first-order adjusted influence measure $FIC_{f(\tilde{\omega}^0),\mathbf{h}}$ at ω^0 in a unit direction \mathbf{h} can be defined as

$$(3.4) \quad FIC_{f(\tilde{\omega}^0),\mathbf{h}} = \mathbf{h}^\top \mathbf{B} \mathbf{h},$$

where $\mathbf{B} = \mathbf{Q}/\text{tr}(\mathbf{Q})$, and $\mathbf{Q} = \mathbf{G}^{-1/2} \nabla_f W_f \nabla_f^\top \mathbf{G}^{-1/2}$.

Next, we decompose \mathbf{B} to obtain non-zero eigenvalues λ and their corresponding eigenvectors e . We utilize the eigenvector e_1 associated with the largest eigenvalue λ_1 to assess the magnitude of the perturbation. As discussed by [Zhu et al. \(2011\)](#), we set $\bar{M}(0) + 2SM(0)$ as a benchmark, where $\bar{M}(0)$ and $SM(0)$ represent the mean and standard error of the values of $M(0)_j$, where $M(0)_j$ is the j -th element along the main diagonal of \mathbf{B} .

3.2.2. Second-order influence measure

If $\nabla_f = 0$, we can measure the Bayesian local influence. By utilizing Taylor expansion, we have $f(\omega(t)) = f(\omega(0)) + \frac{1}{2} f_h''(0) t^2 + O(t^3)$, where $f_h''(0) = \mathbf{h}^\top H_f \mathbf{h}$, and $H_f = \partial_\omega^2 f(\omega(0))$. Now, similar to [Zhu et al. \(2011\)](#), we define the second-order influence measure (SI) in the direction $\mathbf{h} \in \mathcal{R}^m$'s:

$$SI_{f,\mathbf{h}} = SI_{f(\omega(0)),\mathbf{h}} = \frac{\mathbf{h}^\top H_f \mathbf{h}}{\mathbf{h}^\top \mathbf{G} \mathbf{h}},$$

Particularly, for an appropriate perturbation $\tilde{\omega}(\omega)$, $SI_{f,\mathbf{h}}$ is denoted by

$$SI_{f(\tilde{\omega}),\mathbf{h}}|_{\tilde{\omega}=\omega^0} = \frac{\mathbf{h}^\top \mathbf{G}^{-1/2} H_f \mathbf{G}^{-1/2} \mathbf{h}}{\mathbf{h}^\top \mathbf{h}}.$$

Similar to the discussed first-order influence measure, we can denote that

$$(3.5) \quad SIC_{f(\tilde{\omega}^0),\mathbf{h}} = \mathbf{h}^\top \mathbf{B}_s \mathbf{h},$$

where $\mathbf{B}_s = \mathbf{Q}_s/\text{tr}(\mathbf{Q}_s)$, $\mathbf{Q}_s = \mathbf{G}^{-1/2} H_f \mathbf{G}^{-1/2}$.

Similar to the first-order influence measure, the diagonal elements of matrix \mathbf{B}_s are used to identify modeling assumptions with a priori hypotheses of anomalies, unreasonable model assumptions, and abnormal data values. We adopt the same method and benchmark as before. Based on this theoretical foundation, we systematically introduce three objective functions in the following subsection.

3.2.3. Bayes Factor

In the context of Bayes factor, the distance between ω and ω^0 is: $BF(\omega) = \log(p(Y|\omega)) - \log(p(Y|\omega^0))$, and $p(y|\omega) = \int p(y, \theta|\omega) d\theta$. When $W_f = I$, we can get that

$$(3.6) \quad \nabla_{BF} = \mathbb{E}_{p(y, \theta|\omega^0)} (\partial_\omega \log(p(y, \theta|\omega^0))), \quad h_{max}^{BF} = \frac{\mathbf{G}(\omega^0)^{-1/2} \nabla_{BF}}{\sqrt{\nabla_{BF}^\top \mathbf{G}(\omega^0)^{-1} \nabla_{BF}}},$$

so we need to compute $\nabla_{BF} \approx \frac{1}{N} \sum_{n=1}^N \log(p(y, \theta^{(n)}|\omega^0))$, and $\theta^{(n)}$ is sampled from $p(\theta|y, \omega^0)$ by MCMC.

3.2.4. ϕ Divergence

If we consider $f(\omega)$ as the ϕ divergence between two posterior distributions under ω and ω^0 , defined as $D_\phi(\omega) = \int \phi(R(\theta|\omega)) p(\theta|y) d\theta$, and $\phi(\cdot)$ is a convex function with $\phi(1) = 0$. If $\phi(\cdot)$ is $\log(\cdot)$, then ϕ divergence converts to K-L divergence. Moreover, if we represent a as a column vector $\mathbf{a} = [a_1, a_2, \dots, a_n]^\top$, we have $\mathbf{a}^{\otimes 2} = \mathbf{a}\mathbf{a}^\top$.

$$\begin{aligned} H_\phi &= \phi''(1) \mathbb{E}_{\omega^0} \{ \partial_\omega \log(p(\theta|y, \omega^0)) \}^{\otimes 2} \\ &= \phi''(1) E_{\omega^0} \{ \partial_\omega \log(p(y, \theta|\omega^0)) - E_{\omega^0}(\partial_\omega \log(p(y, \theta|\omega^0))) \}^{\otimes 2} \\ &= \phi''(1) [E_{\omega^0} \{ \partial_\omega \log(p(y, \theta|\omega^0)) \}^{\otimes 2} - \{ E_{\omega^0}(\partial_\omega \log(p(y, \theta|\omega^0))) \}^{\otimes 2}], \end{aligned}$$

like Bayes Factor, H_ϕ can also be approximately computed.

$$(3.7) \quad H_\phi \approx \phi''(1) \left[\frac{1}{N} \sum_{n=1}^N \{ \partial_\omega \log(p(y, \theta^{(n)}|\omega^0)) \}^{\otimes 2} - \left(\frac{1}{N} \sum_{n=1}^N \partial_\omega \log(p(y, \theta^{(n)}|\omega^0)) \right)^{\otimes 2} \right],$$

and $\theta^{(n)}$ is sampled by MCMC.

3.2.5. Posterior Mean

The posterior mean of a function $h(\theta)$ can be defined as follows: $M_h(\omega) = \int h(\theta) p(\theta|y, \omega) d\theta$. To quantify the impact of w on the posterior mean of $h(\theta)$ using Cook's posterior mean distance, we measure the difference between the posterior mean $M_h(\omega)$ and the posterior mean $M_h(\omega_0)$, denoted as

$$CM_h(\omega) = (M_h(\omega) - M_h(\omega^0))^\top \mathbf{G}_h (M_h(\omega) - M_h(\omega^0)),$$

where $\mathbf{G}_h = [Var(h(\theta)|y)]^{-1}$. If $f(\omega) = CM_h(\omega)$, we have $\nabla_h = 0$, then we can get $H_h = M_h^{*\top} \mathbf{G}_h M_h^*$, where $M_h^* = Cov_{\omega^0} \{ h(\theta), \partial_\omega \log(p(y, \theta|\omega^0)) \}$. It can be approximately

computed that

$$(3.8) \quad M_h^* = \frac{1}{N} \sum_{n=1}^N \left\{ h(\theta^{(n)}) \partial_\omega \log(p(y, \theta^{(n)} | \omega^0)) \right\} - \left(\frac{1}{N} \sum_{n=1}^N h(\theta^{(n)}) \right) \left(\frac{1}{N} \sum_{n=1}^N \partial_\omega \log(p(y, \theta^{(n)} | \omega^0)) \right),$$

and $\theta^{(n)}$ are also sampled from MCMC.

4. Simulation Studies

4.1. Effectiveness

4.1.1. Example 1

In the previous discussion, we have thoroughly explored the theoretical background of Bayesian local influence analysis in the context of the skew-normal autoregressive model. Now, we simulate the SNAR model to demonstrate the effectiveness of Bayesian local influence analysis. In the simulation, we consider an SNAR(1) model denoted as

$$(4.1) \quad y_t = \beta y_{t-1} + u_t, \quad u_t \sim \text{SN}(0, \sigma^2, \lambda),$$

with parameters $\beta = 0.4$, $\sigma = 1$ and $\lambda = 0.9$. We generate 500 observations based on this model and introduce outliers by modifying y_t to $y_t + 5\sigma$ at $t = 150$ and $t = 400$.

Next, assuming the hyperparameters of the prior distribution are set as follows: $\mu_\beta = \mu_\lambda = 0$, $\sigma_\beta = \sigma_\lambda = 5$, and $n = 10$, we use the MCMC algorithm to construct a Markov chain and obtain 10,000 parameter samples for $\theta = \{\beta, \lambda, \sigma\}$. We discard the first 5,000 samples and retain 5,000 parameter samples for computing the three objective functions described in subsection 3.2.

In Bayesian local influence analysis, the variance perturbation model is a commonly used method that assesses the model's sensitivity to data by changing the size of the standard deviation in the model. The prior-variance perturbation model, on the other hand, focuses on adjusting the variance of the prior distribution to evaluate the model's sensitivity to prior assumptions. We establish a benchmark based on the descriptions in subsections 3.2.1 and 3.2.2 and evaluate the influence measurement using the three objective functions proposed in section 3 (Bayes factor, ϕ divergence, and posterior mean). Points exceeding the benchmark are identified as outliers. The results are shown in the figures below.

In Figures 1 (a), (b) and (c), it can be clearly observed that in the case of variance perturbation, all three measurement metrics (Bayes factor, ϕ divergence, and posterior mean) exhibit significantly higher values at time points $t = 150$ and $t = 400$ compared to other time points, accurately identifying the predetermined perturbation points.

In Figures 1 (d), (e) and (f), simultaneous perturbations in variance and prior are applied. To test whether the Bayesian local influence measure can detect improper prior

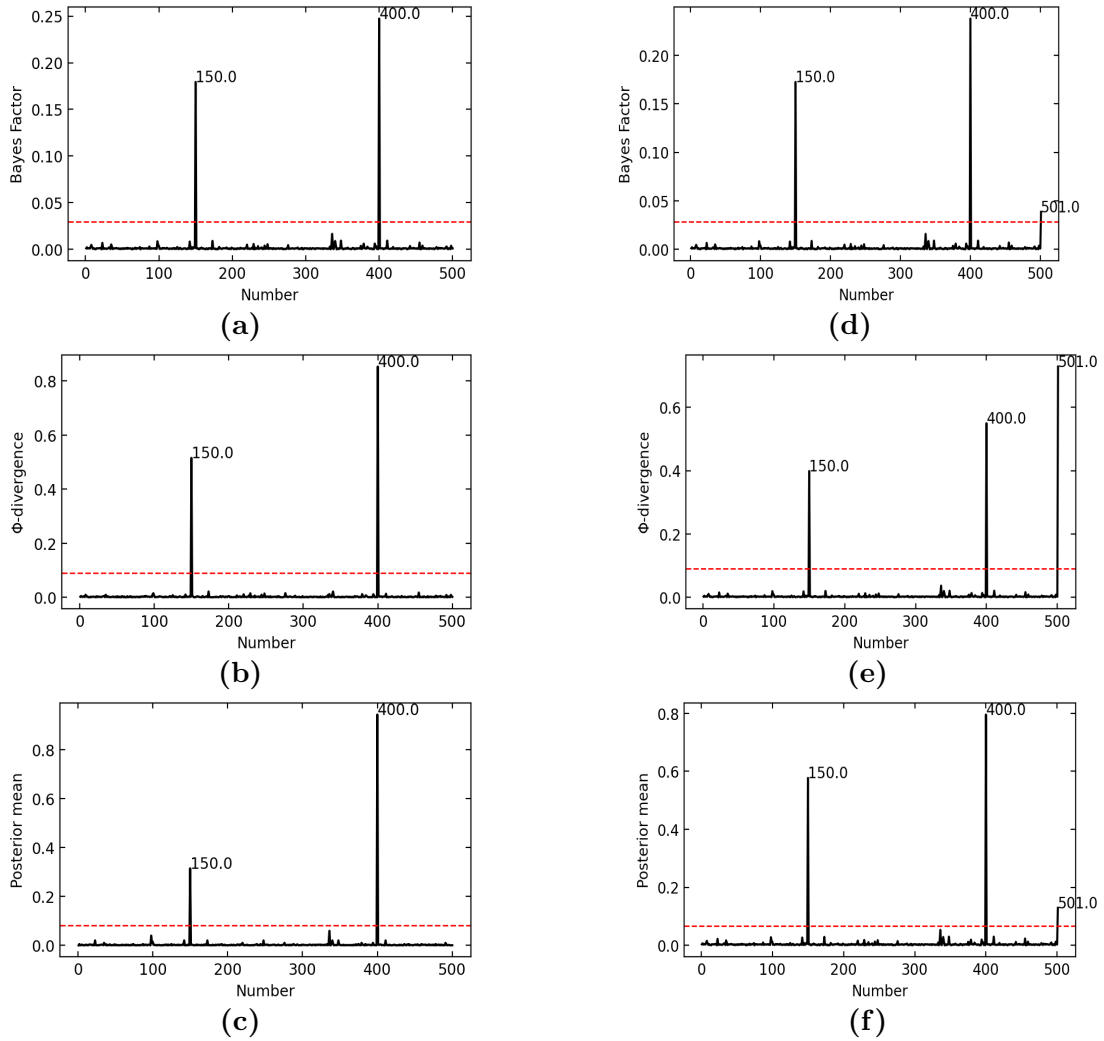


Figure 1: Bayesian local influence on the SNAR model. The three plots on the left (a), (b) and (c) represent the model’s response to perturbations in variance. Conversely, the three plots on the right (d), (e) and (f) depict the model’s response to simultaneous perturbations in variance and prior.

distributions, we perturbed the prior distribution of λ while maintaining the variance perturbation. Specifically, the prior distribution of λ is modified to $N(\mu_\lambda, 0.5\sigma_\lambda^2)$, while the priors of other parameters remain unchanged. In the plots, the first 500 values help identify whether the observations are abnormal, while the values at points 501, 502, and 503 reflect the impact of the prior distributions of λ , σ and β on statistical inference in Bayesian analysis. At point 501, the values are significantly higher than the normal time points, indicating that the perturbation in the prior distribution is successfully detected through Bayesian local influence analysis. These findings demonstrate that the Bayesian local influence method is capable of accurately diagnosing perturbations, both in the case of variance perturbation and simultaneous perturbation of variances and priors.

4.1.2. Example 2

In the previous section, we have experimentally verified the diagnostic effectiveness of Bayesian local influence analysis in one-dimensional time series. The results demonstrate its significant effectiveness in capturing anomalous changes and perturbation points. However, to further evaluate the applicability and stability of this method in higher-dimensional and more complex models, we simulate a SNAR(2) model for more in-depth experimental analysis. Firstly, we consider an SNAR(2) model denoted as

$$(4.2) \quad y_t = \beta_1 y_{t-1} + \beta_2 y_{t-2} + u_t, \quad u_t \sim \text{SN}(0, \sigma^2, \lambda)$$

with parameters $\beta_1 = 0.4$, $\beta_2 = 0.4$, $\sigma = 0.25$ and $\lambda = 0.1$. At time points $t = 150$ and 400 , the simulated y_t values were modified to $y_t + 10\sigma$, constructing the Bayesian perturbation manifold. Sampling calculation and baseline establishment were performed using the same method as Example 1. The diagnostic results are as follows.

From Figures 2 (a), (b) and (c), it can be observed that in the presence of only data perturbations, both the Bayesian local influence analysis methods diagnosed the perturbation points at $t=150$ and 400 . Except for the points at $t=150$ and $t=400$, the values at other time points are relatively small, which reflects the effectiveness of the diagnosis.

In Figures 2 (d), (e) and (f), the approach of simultaneously perturbing both the data and the prior is adopted. While maintaining the data perturbation, the prior for λ is also perturbed. Under unchanged prior conditions for other parameters, the prior for λ is modified to $N(\mu_\lambda, 0.5\sigma_\lambda^2)$. By observing Figures 2 (d), (e) and (f), it is evident that, apart from the points at 150 and 400, the point corresponding to parameter λ at 501 is significantly higher, indicating the effectiveness of the diagnostic method.

4.2. Comparative Analysis

In the previous discussion, we have demonstrated the effectiveness of Bayesian local influence analysis in a SNAR model. Therefore, in this subsection, we will compare this model with other models. We will conduct two types of comparative studies. The first type involves generating data from the SNAR(1) model mentioned in Example 1. We will construct both a skew-normal AR model and a normal AR model based on this dataset and compare the strengths and weaknesses of the Bayesian local influence analysis method in diagnosing these two models. The second type of comparison still involves generating data from the SNAR(1) model shown in Example 1. We will compare the performance of the Bayesian local influence analysis method and the local influence analysis method in diagnosing the same model.

We will perform the comparisons following these steps:

Step 1. Construct an AR model where the errors follow a skew-normal distribution.

Step 2. Generate a set of time series y_t with a sample size of 500 using the model specified in Step 1.

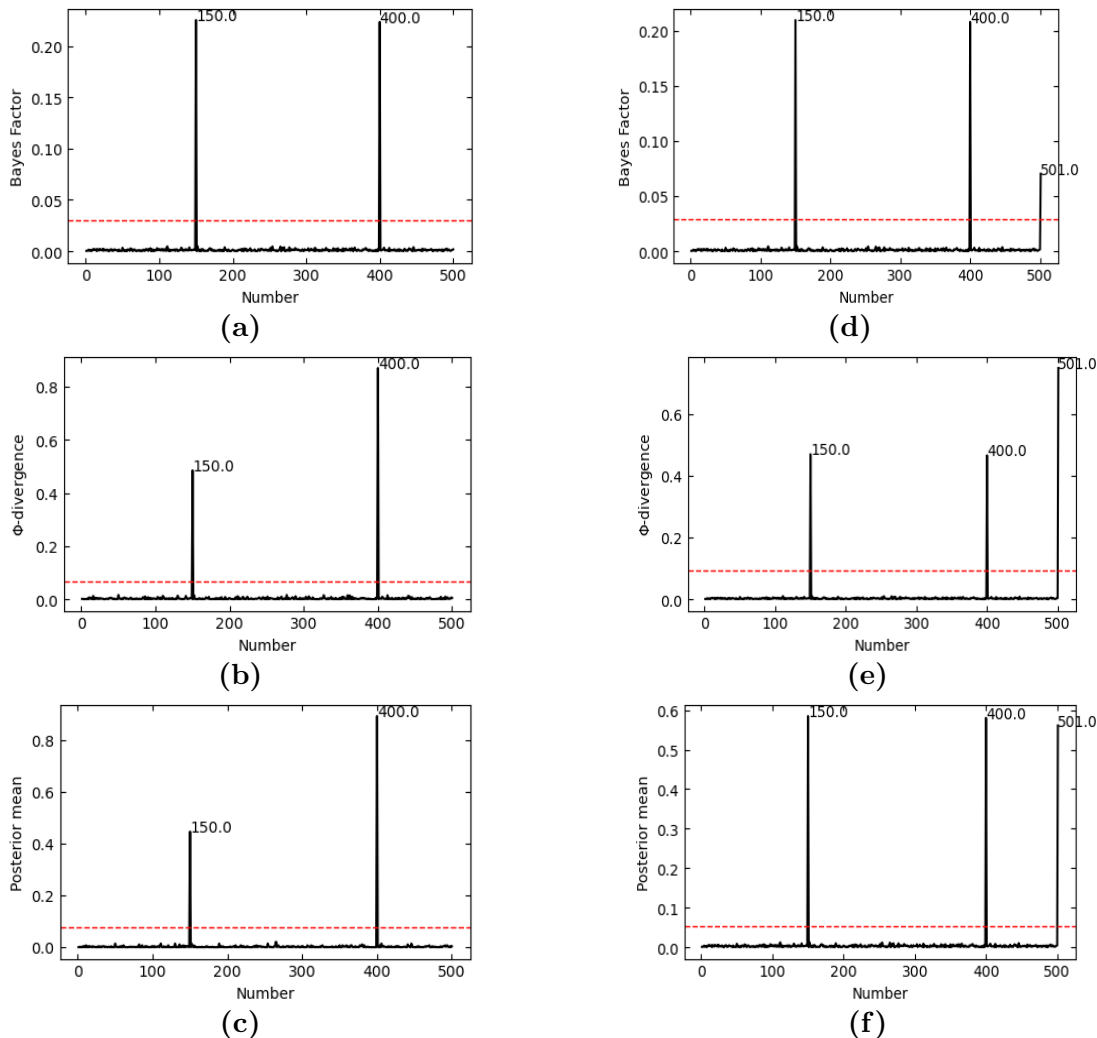


Figure 2: Bayesian local influence on the SNAR model. The three plots on the left (a), (b) and (c) represent the model’s response to perturbations in data. Conversely, the three plots on the right (d), (e) and (f) depict the model’s response to simultaneous perturbations in data and prior.

Step 3. Conduct variance and data perturbations like subsection 4.1.1 and 4.1.2 in $y_{100}, y_{200}, y_{300}, y_{400}$.

Step 4. Detect outliers employing three objective functions in model built in Step 3.

Step 5. Repeat Step 2 to Step 4 for 1000 times to obtain the detected outliers.

Finally, we compare and analyze the diagnostic results of the Normal Autoregressive (NAR) and Skew-Normal Autoregressive (SNAR) models based on 4,000 outlier points. The table reports the number of outliers detected by various theoretical methods under two different perturbation schemes.

From Table 1, it is seen that when simulating data as skewed data, the diagnostic performance of establishing an AR model with residuals following a skew-normal distribution is better than establishing an AR model with residuals following a normal distribution. Based

Table 1: Comparison of detected outliers across perturbation schemes for NAR and SNAR models

Model	Perturbation of sd's	Perturbation of data
SNAR Model	1962	2038
NAR Model (Bayes Factor)	3387	3400
NAR Model (ϕ Divergence)	1979	1790
NAR Model (Posterior Mean)	2652	2711
SNAR Model (Bayes Factor)	3241	2571
SNAR Model (ϕ Divergence)	2340	1953
SNAR Model (Posterior Mean)	3241	2910

on the number of outliers detected in the NAR and SNAR models, two (ϕ divergence and posterior mean) out of the three measurement scales (Bayes factor, ϕ divergence and posterior mean) show more accurate outlier detection under the assumption of a skew-normal distribution. This indicates that establishing a NAR Model for data generated by a SNAR model may not necessarily allow the Bayesian local influence method to diagnose the corresponding perturbation points. Furthermore, we recognise that both local influence analysis and Bayesian local influence analysis are effective in the case of a SNAR model. The first row in Table 1 represents the SNAR model. In the local influence analysis, the SNAR model identifies 1,962 and 2,038 outliers in the variance disturbance model and the data disturbance model, respectively. However, in terms of the number of detected outliers, the three measures of the Bayesian local influence method generally outperform the diagnostic effectiveness of the local influence analysis method, regardless of whether it is in the context of perturbing the variance or the data.

5. Empirical Study

For the Chinese stock market, 2015 was a turbulent year, marked by a severe crash that significantly impacted investors and the economy. From 2014 to early 2015, the market experienced a strong upward trend, driven by government policies encouraging investment and a surge in retail participation, which led to rapid price increases. However, the widespread use of margin financing amplified market risks, as heavily leveraged investors sought higher returns, leading to increased volatility. Regulatory measures proved ineffective in stabilizing the market, further heightening investor concerns. By mid-June 2015, the market sharply declined, triggering panic selling and causing the Shanghai Composite Index and Shenzhen Component Index to plummet by nearly 40% and 50%, respectively, resulting in significant losses in market capitalization.

The stock market crash severely undermined investor confidence and economic activity, leading to reduced investment and consumption. This downturn also posed risks to China's financial system by increasing the likelihood of systemic repercussions. To assess the applicability of Bayesian local influence analysis in detecting market instability, we analyzed daily log returns of the Shanghai Composite Index from January 5 to December 31, 2015. The dataset, obtained from the Wind database, consists of 243 observations. The following section presents key statistical summaries and kernel density estimates to provide deeper

insights into market behavior during this period.

Table 2: Basic statistics of the daily logarithmic returns of the Shanghai Composite Index

Sample size	Minimum	Maximum	1st quartile	3rd quartile	Mean
243	-0.0887	0.0560	-0.0113	0.0161	0.0002
Median	Variance	Standard Deviation	Skewness	Kurtosis	Interquartile Range
0.0026	0.0006	0.0246	-0.9370	2.0078	0.0274

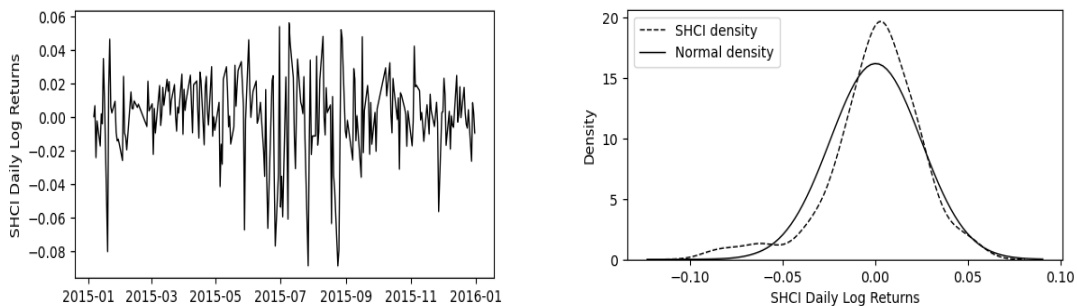


Figure 3: Shanghai Composite Index daily logarithmic returns data and kernel density estimation plot

From Table 2 and Figure 3, it is evident that fitting the daily logarithmic returns of the Shanghai Composite Index with a normal distribution is clearly insufficient. The selected data exhibit characteristics such as peakedness, fat tails, and asymmetry, which are common in the majority of financial data. However, a skewed normal distribution is well-suited to capture these features. Therefore, we consider using a skewed normal distribution to fit this data.

Figure 3 displays the daily logarithmic returns of the Shanghai Composite Index. After conducting the Augmented Dickey-Fuller (ADF) test and Ljung-Box Q-test with a lag order of 12, both results reject the null hypothesis at the 1% significance level. This indicates that the data form a stationary, non-white noise time series, suggesting the potential for further time series modeling. From Figure 4, the partial autocorrelation structure suggests that an AR(2) model may be suitable for capturing the linear dependence in the data. After fitting the AR(2) model, a lag-12 Q-test on the residuals yields a test statistic of 14.5378 with a p-value of 0.2677. Therefore, we cannot reject the null hypothesis that the residuals are uncorrelated. While this supports the adequacy of the AR(2) model in capturing the linear structure, we acknowledge that uncorrelated residuals do not necessarily imply white noise, as homoscedasticity is also required. Nevertheless, the AR(2) model appears to provide a reasonable fit to the data.

Next, we fit an SNAR(2) model to the data and, following the local influence framework in Liu et al. (2020b, 2024a), construct four perturbation schemes – Case-weight, Data, Variance, and Skewness – to detect potential outliers using the classical approach. Assuming the prior distributions $\beta \sim \mathcal{N}(0, 5)$, $\lambda \sim \mathcal{N}(0, 5)$, and $\sigma \sim \chi^2(1)$, we apply the MCMC algorithm from Section 2 to estimate the model parameters. Under the Bayesian local influence

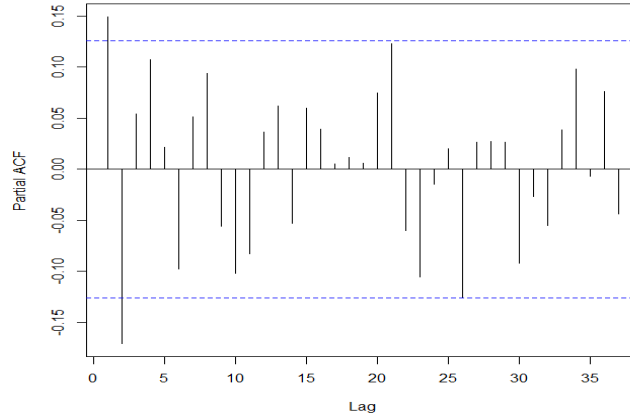


Figure 4: PACF of daily logarithmic returns for the Shanghai Composite Index

framework, abnormal observations are identified using three objective functions: the Bayes factor, ϕ divergence, and the posterior mean. Table 3 summarizes the results, where an asterisk (*) indicates days when the daily logarithmic return of the Shanghai Composite Index was identified as an outlier by the respective method.

Table 3: Summary of abnormal points detected for daily log returns of Shanghai Composite Index

Date	Observed value	Case-weight	Data	Variance	Skewness	Bayes factor	ϕ divergence	Posterior mean
19/01/2015	-8.02%	*	*	*	*	*	*	*
28/05/2015	-6.73%	*	*		*	*	*	*
18/06/2015	-3.74%							*
19/06/2015	-6.63%		*	*	*	*		*
26/06/2015	-7.68%	*	*	*	*	*	*	*
30/06/2015	5.38%							*
01/07/2015	-5.37%	*	*		*	*	*	*
03/07/2015	-5.95%	*	*	*	*	*	*	*
08/07/2015	-6.08%		*		*			
09/07/2015	5.60%	*	*		*	*		*
27/07/2015	-8.86%	*	*	*	*	*	*	*
18/08/2015	-6.34%	*	*		*	*		*
24/08/2015	-8.87%	*	*	*	*	*	*	*
25/08/2015	-7.94%	*	*	*	*	*		
16/09/2015	4.78%							*
27/11/2015	-5.64%		*		*			*

The provided text describes the effectiveness of local influence analysis and Bayesian local influence analysis in practical applications, specifically related to the Chinese stock market crash of 2015. The analysis demonstrates that the majority of diagnosed anomalies were concentrated between June and August, corresponding to the actual occurrence of the stock market crash.

Moreover, the diagnostic rate increases as the Shanghai Composite Index experiences greater volatility, indicating a higher likelihood of being diagnosed. This observation suggests that during periods of high market volatility, both local influence analysis and Bayesian local

influence analysis perform well in detecting anomalies.

To illustrate this point, specific events are mentioned. On January 19, 2015, major securities firms were punished by the China Securities Regulatory Commission for violations in margin financing and securities lending. Additionally, the China Banking Regulatory Commission issued regulations on the direction of credit flow. These events were misinterpreted by investors, leading to panic selling and a significant drop in the Shanghai Composite Index. Both local influence and Bayesian local influence analyses were effective in detecting this anomaly.

However, when dealing with anomalies characterized by smaller fluctuations, Bayesian local influence analysis demonstrates superior diagnostic capability. For instance, on June 18, 2015, June 30, 2015, and September 16, 2015, when the Shanghai Composite Index exhibited minimal volatility, regular local influence analysis failed to diagnose these anomalies. In contrast, Bayesian local influence analysis successfully identified them. These specific dates mark significant milestones for the Shanghai Composite Index.

Overall, the analysis highlights the performance of local influence analysis and Bayesian local influence analysis in detecting anomalies in the Chinese stock market, particularly during the turbulent period of the 2015 stock market crash.

6. Concluding Remarks

In summary, this paper focuses on the Bayesian statistical diagnostics problem of autoregressive (AR) models under the assumption of a skew-normal distribution. The parameter estimation of AR models under the skew-normal distribution is achieved using the MCMC algorithm. Subsequently, the Bayesian local influence analysis method is applied to statistically diagnose the models by considering three types of disturbances: priors, variances, and data. The objective functions used in the analysis are Bayes factor, ϕ divergence, and posterior mean.

Numerical simulations are conducted to verify the effectiveness of the proposed method and demonstrate its superiority over traditional local influence analysis. The results show that the Bayesian local influence analysis method outperforms the traditional approach, particularly for extremal observations with smaller fluctuations.

In the empirical section, the daily log returns of the Shanghai Composite Index in 2015 are modeled using the skew-normal distribution for AR modeling. The findings indicate that the Bayesian local influence analysis method exhibits better performance in detecting extremal observations compared to traditional approaches.

Furthermore, the Bayesian statistical diagnostic method proposed in this paper has the potential to be extended to more complex models, such as autoregressive models with scale mixtures of skew-normal (SMSN-AR), skew-t, and other distributions, as well as multivariate autoregressive (MAR) models. This expansion would enable its application to a broader range of practical scenarios. Exploring these extensions represents a crucial direction for our future research.

ACKNOWLEDGMENTS

We would like to sincerely thank the Reviewers and Editors for their constructive and insightful comments, which have significantly improved the presentation of our manuscript. Yonghui Liu gratefully acknowledges the support of the National Social Science Foundation of China (22&ZD160) for this research. Shuangzhe Liu appreciates the University of Canberra for supporting his research leave in 2024.

REFERENCES

- Azzalini, A. (1985). A class of distributions which includes the normal ones. *Scandinavian Journal of Statistics*, 12(2):171–178.
- Azzalini, A. (2013). *The Skew-normal and Related Families*. Cambridge University Press., Cambridge, UK.
- Box, G. E. P., Jenkins, G. M., Reinsel, G. C., and Ljung, G. M. (2015). *Time Series Analysis: Forecasting and Control*. John Wiley & Sons, Hoboken, NJ, 5th edition.
- Cao, C. Z., Lin, J. G., and Shi, J. Q. (2014). Diagnostics on nonlinear model with scale mixtures of skew-normal and first-order autoregressive errors. *Statistics*, 48(5):1033–1047.
- Cárcamo, E., Marchand, C., Ibacache-Pulgar, G., and Leiva, V. (2024). Birnbaum–saunders semi-parametric additive modeling: estimation, smoothing, diagnostics, and application. *REVSTAT – Statistical Journal*, 22(2):211–237.
- Carmichael, B. and Coën, A. (2013). Asset pricing with skewed-normal return. *Finance Research Letters*, 10(2):50–57.
- Chen, C. W., So, M. K., and Gerlach, R. H. (2005). Asymmetric response and interaction of US and local news in financial markets. *Applied Stochastic Models in Business and Industry*, 21:273–288.
- Cook, R. (1986). Assessment of local influence. *Journal of the Royal Statistical Society Series B: Statistical Methodology*, 48(2):33–155.
- Dai, X., Jin, L., Tian, M., and Shi, L. (2019). Bayesian local influence for spatial autoregressive models with heteroscedasticity. *Statistical Papers*, 60:1423–1446.
- Dang, W., Zhu, F., Xu, N., and Liu, S. (2025). Diagnostic analytics for the mixed poisson ingarch model with applications. *Journal of Applied Statistics*. Published online: 12 March 2025.
- Fama, E. F. (1965). The behavior of stock-market prices. *The Journal of Business*, 38(1):34–105.
- Ju, Y., Tang, N., and Li, X. (2018). Bayesian local influence analysis of skew-normal spatial dynamic panel data models. *Journal of Statistical Computation and Simulation*, 88:2342–2364.
- Ju, Y., Yang, Y., Hu, M., Dai, L., and Wu, L. (2022). Bayesian influence analysis of the skew-normal spatial autoregression models. *Mathematics*, 10(8):1306.
- Lawrance, A. J. (1988). Regression transformation diagnostics using local influence. *Journal of the American Statistical Association*, 83(404):1067–1072.
- Lesaffre, E. and Verbeke, G. (1998). Local influence in linear mixed models. *Biometrics*, 54:570–582.
- Liu, S. (2000). On local influence for elliptical linear models. *Statistical Papers*, 41:211–224.

- Liu, S. (2004). On diagnostics in conditionally heteroskedastic time series models under elliptical distributions. *Journal of Applied Probability*, 41A:393–405.
- Liu, S., Leiva, V., Zhuang, D., Ma, T., and Figueroa-Zúñiga, J. I. (2022a). Matrix differential calculus with applications in the multivariate linear model and its diagnostics. *Journal of Multivariate Analysis*, 188:104849.
- Liu, T., Liu, S., and Shi, L. (2020a). *Time Series Analysis using SAS Enterprise Guide*. Springer Singapore.
- Liu, Y., Ji, G., and Liu, S. (2015). Influence diagnostics in a vector autoregressive model. *Journal of Statistical Computation and Simulation*, 85(13):2632–2655.
- Liu, Y., Mao, C., Leiva, V., Liu, S., and Silva Neto, W. A. (2022b). Asymmetric autoregressive models: Statistical aspects and a financial application under COVID-19 pandemic. *Journal of Applied Statistics*, 49(5):1323–1347.
- Liu, Y., Mao, G., Leiva, V., Liu, S., and Tapia, A. (2020b). Diagnostic analytics for an autoregressive model under the skew-normal distribution. *Mathematics*, 8(5):693.
- Liu, Y., Sang, R., and Liu, S. (2017). Diagnostic analysis for a vector autoregressive model under Student's t-distributions. *Statistica Neerlandica*, 71(2):86–114.
- Liu, Y., Wang, J., Leiva, V., Tapia, A., Tan, W., and Liu, S. (2024a). Robust autoregressive modeling and its diagnostic analytics with a COVID-19 related application. *Journal of Applied Statistics*, 51(7):1318–1343.
- Liu, Y., Wang, J., Yao, Z., Liu, C., and Liu, S. (2024b). Diagnostic analytics for a GARCH model under skew-normal distributions. *Communications in Statistics-Simulation and Computation*, 53:4850–4874.
- Makowski, D., Wallach, D., and Tremblay, M. (2002). Using a bayesian approach to parameter estimation; comparison of the GLUE and MCMC methods. *Agronomie*, 22(2):191–203.
- Maleki, M. and Arellano-Valle, R. B. (2017). Maximum a-posteriori estimation of autoregressive processes based on finite mixtures of scale-mixtures of skew-normal distributions. *Journal of Statistical Computation and Simulation*, 87(6):1061–1083.
- McCulloch, R. E. (1989). Local model influence. *Journal of the American Statistical Association*, 84(406):473–478.
- McCulloch, R. E. and Tsay, R. S. (1994). Bayesian analysis of autoregressive time series via the gibbs sampler. *Journal of Time Series Analysis*, 15(2):235–250.
- Paula, G. A., Leiva, V., Barros, M., and Liu, S. (2012). Robust statistical modeling using the birnbaum-saunders-t distribution applied to insurance. *Applied Stochastic Models in Business and Industry*, 28(1):16–34.
- Peiro, A. (1999). Skewness in financial returns. *Journal of Banking & Finance*, 23(6):847–862.
- Saavedra-Nievas, J. C., Nicolis, O., Galea, M., and Ibacache-Pulgar, G. (2023). Influence diagnostics in gaussian spatial-temporal linear models with separable covariance. *Environmental and Ecological Statistics*, 30:131–155.
- Su, Z., Zhu, F., and Liu, S. (2024). Local influence analysis in the softplus ingarch model. *TEST*, 33:951–985.
- Zhu, F., Liu, S., and Shi, L. (2016). Local influence analysis for poisson autoregression with an application to stock transaction data. *Statistica Neerlandica*, 70(1):4–25.
- Zhu, F., Shi, L., and Liu, S. (2015). Influence diagnostics in log-linear integer-valued garch models. *AStA Advances in Statistical Analysis*, 99:311–335.

Zhu, H., Ibrahim, J. G., and Tang, N. (2011). Bayesian influence analysis: a geometric approach. *Biometrika*, 98(2):307–323.

Zhu, H. T. and Lee, S. Y. (2001). Local influence for incomplete data models. *Journal of the Royal Statistical Society: Series B: Statistical Methodology*, 63(1):111–126.